associated with phase diffusion brought about by a random noise perturbation due to thermal fluctuations. In the quantum theory, the process of contraction of the density matrix after the decay of each injected atom would convert even a pure case into a mixture, so that Eqs. (2) really describe an ensemble of lasers for which phase information is gradually lost. The density matrix does not describe the laser but rather our state of knowledge of the ensemble of lasers under consideration. If we knew initially that a single laser had a nonvanishing electric field, a density matrix with nonzero off-diagonal elements would be required for the initial description, and the average electric field would only decay with the very long mean life of $1/D$.

*Research supported in part by the National Aeronautics and Space Administration and by the U. S. Air Force Office of Scientific Research.

[1]W. E. Lamb, Jr., Phys. Rev. 134, A1429 (1964).

[2]W. E. Lamb, Jr., in Proceedings of the International School of Physics "Enrico Fermi," Course XXXI, edited by P. A. Miles (Academic Press, Inc., New York, 1964), p. 78.

[3]W. E. Lamb, Jr., in Quantum Optics and Electronics; Lectures Delivered at Les Houches During the 1964 Session of the Summer School of Theoretical Physics, University of Grenoble, edited by C. De Witt, A. Blandin, and C. Cohen-Tannoudji (Gordon and Breach Publishers, Inc., New York, 1965).

[4]For an alternative approach see M. Scully, W. E. Lamb, Jr., and M. J. Stephen, in Proceedings of the International Conference on the Physics of Quantum Electronics, Puerto Rico, 1965, edited by P. L. Kelley, B. Lax, and P. E. Tannenwald (McGraw-Hill Book Company, Inc., New York, 1965), p. 759. (In this work only the lowest order terms in B were kept.)

[5]The off-diagonal elements $\rho_{n,n'}$, $n' \neq n$, provide a determination of the frequency of oscillation for the quantum field, which is in agreement with that obtained from the classical field analysis.

[6]Ref. 1, Eq. (175).

[7]The time dependence of $\rho_{n,n}(t)$ will be presented in the form of a moving picture by M. Scully, W. E. Lamb, Jr., and M. Sargent at the Proceedings of the Fourth Quantum Electronics Conference, 1966 (unpublished).

[8]B. Pariser and T. C. Marshall, Appl. Phys. Letters 6, 232 (1965); B. Pariser, thesis, Columbia University, 1965 (unpublished).

[9]The linewidth D is made up of two parts. The terms involving x represent the effects of thermal and electromagnetic vacuum fluctuations in the cavity, and were given by Lamb in Eq. (15.35) of Ref. 3. The terms involving N_a, N_b arise from (spontaneous and induced) emission and absorption by the active atoms.

[10]For the case under consideration, Eq. (9) agrees with the results of M. Lax, in Proceedings of the International Conference on the Physics of Quantum Electronics, Puerto Rico, 1965, edited by P. L. Kelley, B. Lax, and P. E. Tannenwald (McGraw-Hill Book Company, Inc., New York, 1965), p. 735; and V. Korenman, ibid., p. 748.

EXPERIMENTAL STUDY OF $p+p \rightarrow p+N^*$ AT INCIDENT ENERGIES OF 6-30 BeV*

E. W. Anderson, E. J. Bleser, G. B. Collins, T. Fujii,† J. Menes, F. Turkot

Brookhaven National Laboratory, Upton, New York

and

R. A. Carrigan, Jr., R. M. Edelstein, N. C. Hien, T. J. McMahon, and I. Nadelhaft

Carnegie Institute of Technology, Pittsburgh, Pennsylvania

(Received 8 April 1966)

This Letter reports preliminary results of a study of inelastic proton-proton scattering at incident momenta of 6, 10, 15, 20, and 30 BeV/c and squared four-momentum transfers $|t|$ of 0.04 to 5 (BeV/c)^2. The experiment was carried out at the Brookhaven alternating-gradient synchrotron (AGS). Similar studies have have been made at incident momenta up to 3.7 BeV/c at the Cosmotron,[1] up to 7 BeV/c at the Bevatron,[2] and up to 26 BeV/c at CERN.[3] This experiment extends these studies over a very wide range of incident momenta and momentum transfers in order to obtain both detailed information and a qualitative understanding of the behavior of inelastic channels at high energy. Differential cross sections were obtained for the following processes

$$p+p \rightarrow p+N_{3/2,3/2}^*(1.238),$$
$$\rightarrow p+N_{?,?}^*(1.4),$$
$$\rightarrow p+N_{1/2,3/2}^*(1.52),$$
$$\rightarrow p+N_{1/2,5/2}^*(1.69),$$
$$\rightarrow p+N_{1/2,?}^*(2.19),$$

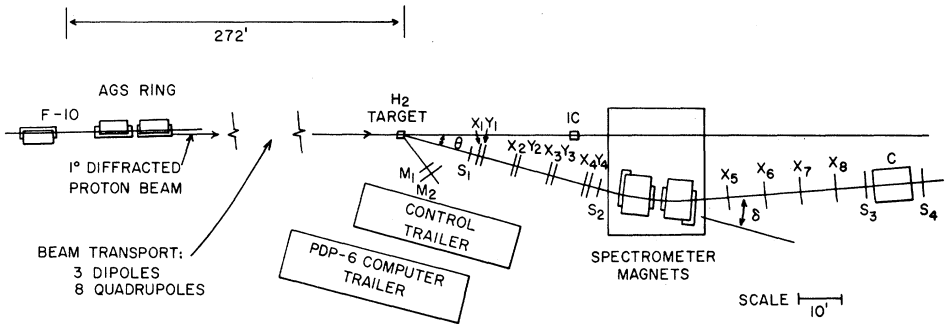

FIG. 1. Experimental layout. X_iY_i are wire chambers to measure horizontal and vertical coordinates along the scattered proton trajectory, C is a Cherenkov counter, the S_i are trigger counters such that a scattered proton event is registered as $S_1S_2S_3S_4\bar{C}$, and M_1M_2 form a beam monitor telescope; these items are not drawn to scale. IC is an ion chamber used to monitor the incident beam. The scattering angle θ was adjustable from 0° to 15°, and the deflection angle δ was varied from 2° to 12°.

where the mass, in BeV, is given in parentheses and the first and second subscripts are the isospin and the spin, respectively.[4]

A magnetic spectrometer,[5] recently developed at Brookhaven, was used to analyze protons scattered by a hydrogen target. The spectrometer made use of wire spark chambers with magnetic-core readout to locate and digitize a number of points along the trajectory of the scattered proton. A plan of the layout is given in Fig. 1. The information from the chambers was coded and sent to a computer (Digital Equipment Corporation PDP-6) which calculated, "on-line," the scattering angle and momentum for each event. At the end of each run a summary was printed out which included histograms of differential cross sections, beam characteristics, and information on the performance of the wire chambers. Data rates ranged from one to 150 events per AGS pulse, depending on the cross section under study. Target-empty rates were typically <5% of target-full rates.

The incident beam was obtained from the AGS circulating beam by diffraction scattering at 1° from an internal beryllium target during a "front porch" which preceded the main flat top of the AGS magnet cycle. The momentum spread in the beam was ±0.25%, the angular divergence was less than 1 mrad, and the intensity could be varied from 10^5 to 10^8 protons per pulse for a circulating intensity of 5×10^{11} protons per pulse. The beam intensity was measured with an ionization chamber and with a counter telescope at 22° looking at the hydrogen target. The over-all momentum resolution for the system, including the beam contribution, was ±0.45% at 6 BeV/c and ±0.3% at 30 BeV/c. The over-all angular resolution was limited by the beam divergence to ±0.4 mrad.

For each event the missing mass was calculated from the momentum and scattering angle of the detected proton. The missing-mass resolution in the 1- to 2-BeV region varied from ±20 MeV at 6 BeV/c to ±60 MeV at 30 BeV/c. A number of representative missing-mass histograms are shown in Figs. 2(a)-2(e). The peaks in Fig. 2 correspond to the elastic peak and to the well-known isobars with masses 1.238, 1.52, and 1.68 BeV, as well as the more recently discovered isobar at 2.19 BeV[6] and the phenomenon at 1.4 BeV.[7]

The qualitative features of the data can be summarized as follows. The $N^*(1.238)$ can be seen at as high an energy as 15 BeV. The phenomenon at 1.4 BeV dominates the inelastic spectrum at high energy and low momentum transfer [$|t|<0.1$ (BeV/c)^2]. The $N^*(1.52)$ is seen consistently for $|t|>0.3$ (BeV/c)^2 but is hard to resolve for $|t|<0.3$ (BeV/c)^2 where the $N^*(1.4)$ is present. In fact, the $N^*(1.4)$ and $N^*(1.52)$ seem to produce a compound peak which shifts in mass from 1.4 to 1.52 BeV as the momentum transfer increases. The $N^*(1.69)$ is present at all energies and momentum transfers. At 20 and 30 BeV/c, where the higher mass range was surveyed, the $N^*(2.19)$ is present. There is no clear evidence for excitation of the isospin-$\frac{3}{2}$ states at 1.92 and at 2.36 BeV.[6] Finally, the dependence of the differential cross sections on incident energy is much less marked than the dependence on momentum transfer.

In order to obtain quantitative measurements of the differential cross sections for the various processes, it is necessary to integrate

the areas under the corresponding peaks and above the background. This procedure has been carried out in two ways: (1) by hand, using a "reasonable" hand-drawn background, and (2) by computer, fitting a sum of Breit-Wigner resonance shapes and a polynomial background function to the data by the method of least squares. It has been assumed that there is no coherent interference among the resonances or with the background. The two procedures give reasonable agreement. There are two types of errors inherent in either fitting procedure. Uncertainties associated with the assumed shapes and widths of the resonance peaks lead to an error of ±50% in the over-all normalization for each isobar. It is expected that these errors will be decreased by more thorough analysis. Secondly, there are statistical errors and uncertainties in the background shape which lead to relative (point-to-point) errors. For most of the data these are smaller than ±25%. For the $N^*(1.24)$ at 15 BeV/c and the $N^*(2.19)$ at both 20 and 30 BeV/c, relative errors of ±50% are quoted because their small amplitudes make the cross sections unusually sensitive to the choice of background. For the $N^*(1.52)$ and $N^*(1.69)$ at $|t|>1.5$ (BeV/c)^2, the errors reflect the large statistical uncertainties.

Our values for $d\sigma/dt$ are given in Figs. 3(a)-3(f) for each channel at the various energies and t values. For comparison, the differential elastic cross sections are also shown.[8]

Since the differential cross sections in Fig. 3 show an exponential dependence on t for $|t|<1.0$ (BeV/c)^2, an expression of the form $d\sigma/dt = Ae^{-b|t|}$ has been fitted to the data. The results are given in Table I, along with the range of t fitted, and are plotted in Fig. 3. Total cross sections, approximated by $2A/b$ (the factor 2 takes account of the backward hemisphere in the center-of-mass system), are also given in Table I and are plotted in Fig. 4 as a function of incident momentum. The errors quoted on A and b arise from the relative errors in the differential cross sections. Errors in the over-all normalization of a particular isobar will affect the values of A but will not affect the momentum-transfer dependence (the slope b) or the energy dependence of A and b for that isobar.

On the basis of the results so far, the following tentative conclusions may be drawn.

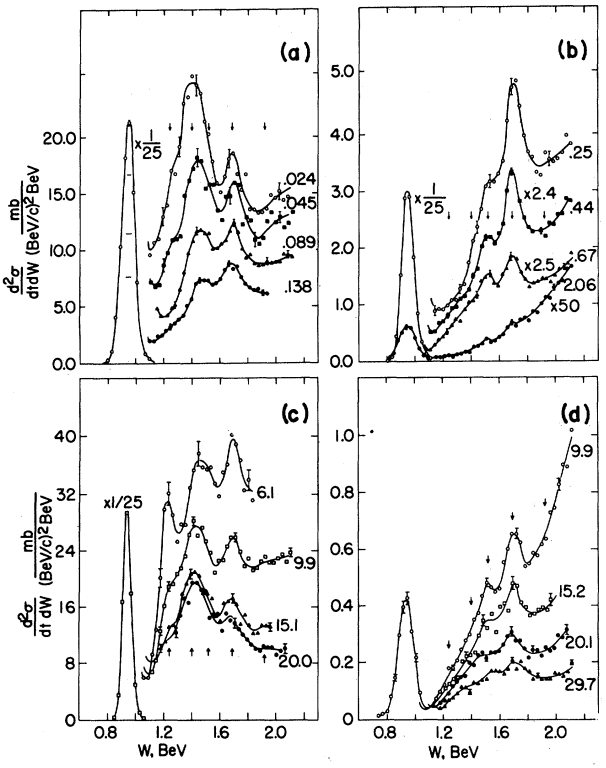

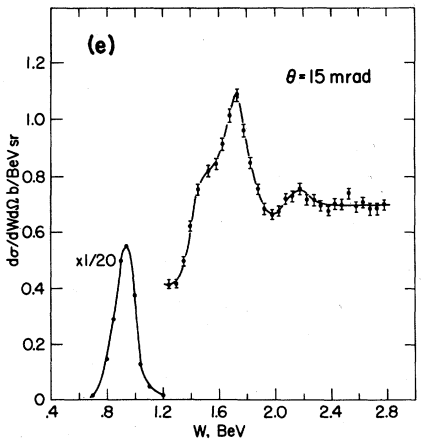

FIG. 2. Typical plots of the doubly differential cross section, $d^2\sigma/(d|t|dW)$, versus W, where $|t|$ is the squared four-momentum transfer and W is the invariant missing mass. The arrows indicate the W values for the isobars of mass 1.238, 1.40, 1.52, 1.69, and 1.92 BeV. (a) and (b) Variation of the cross section as $|t|$ varies from 0.024 to 2.06 (BeV/c)^2 and the incident proton momentum is fixed at 15.1 BeV/c. (c) Variation of the cross section as the incident proton momentum changes from 6.1 BeV/c to 20.0 BeV/c and $|t|$ is fixed at 0.042 (BeV/c)^2. (d) Variation of the cross section as the incident proton momentum changes from 9.9 to 29.7 BeV/c and $|t|$ is fixed at 0.82 (BeV/c)^2. (e) Example of the production of N^* (2.19) at an incident proton momentum of 30 BeV/c and $|t|=0.19$ (BeV/c)^2. In this case only the quantity plotted is $d^2\sigma/dWd\Omega$.

(1) At high energy and very small momentum transfer, the most striking feature is the $N^*(1.4)$. In those cases where it is dominant, its mass is 1.405 ± 0.015 BeV and its width is 180 ± 50 MeV. Recent phase-shift analyses of π-p scattering[9] indicate a possible P_{11} resonance in the mass region of 1.4 to 1.5 BeV, but the evidence is not yet conclusive. If the $N^*(1.4)$ as seen in this experiment is to be identified with anything in πp total cross sections, as are other isobars, its excitation mechanism must be remarkably more efficient than that for the other isobars. Possibly, the Drell-Hiida mechanism plays a role here.[10] Alternatively, it may be that the $N^*(1.4)$ is a highly inelastic resonance and is therefore suppressed in πp total cross sections.

(2) For $|t| < 1.0$ $(\mathrm{BeV}/c)^2$ the slopes of the five differential cross sections under study divide into two sets. The three isospin-$\frac{1}{2}$ isobars with masses 1.52, 1.69, and 2.19 BeV, have a slope of about 5 $(\mathrm{BeV}/c)^{-2}$, which is half the slope of the elastic cross section. The isospin-$\frac{3}{2}$ isobar with mass 1.24 BeV and the phenomenon at 1.40 BeV have a slope of about 15-20 $(\mathrm{BeV}/c)^{-2}$, or twice the slope of the elastic cross section. This variety in the slopes seems inconsistent with the "coherent droplet" model.[11,12]

(3) Table I and Fig. 3(e) indicate that the fitted slope for the 1.69 isobar is about 5 $(\mathrm{BeV}/c)^{-2}$ over the entire energy range. However, the increase in this slope as the energy increases suggests a possible "shrinkage" effect. For $|t| > 1.0$ $(\mathrm{BeV}/c)^2$ the differential cross sections for both the $N^*(1.52)$ and $N^*(1.69)$ show a distinct energy dependence. As can be seen in Figs. 3(d) and 3(e), there is a resemblance to the behavior of the elastic differential cross section in this region, consistent with a speculation of Wu and Yang.[13] The slopes for $|t| > 1$ $(\mathrm{BeV}/c)^2$ average about 1.5 $(\mathrm{BeV}/c)^{-2}$.

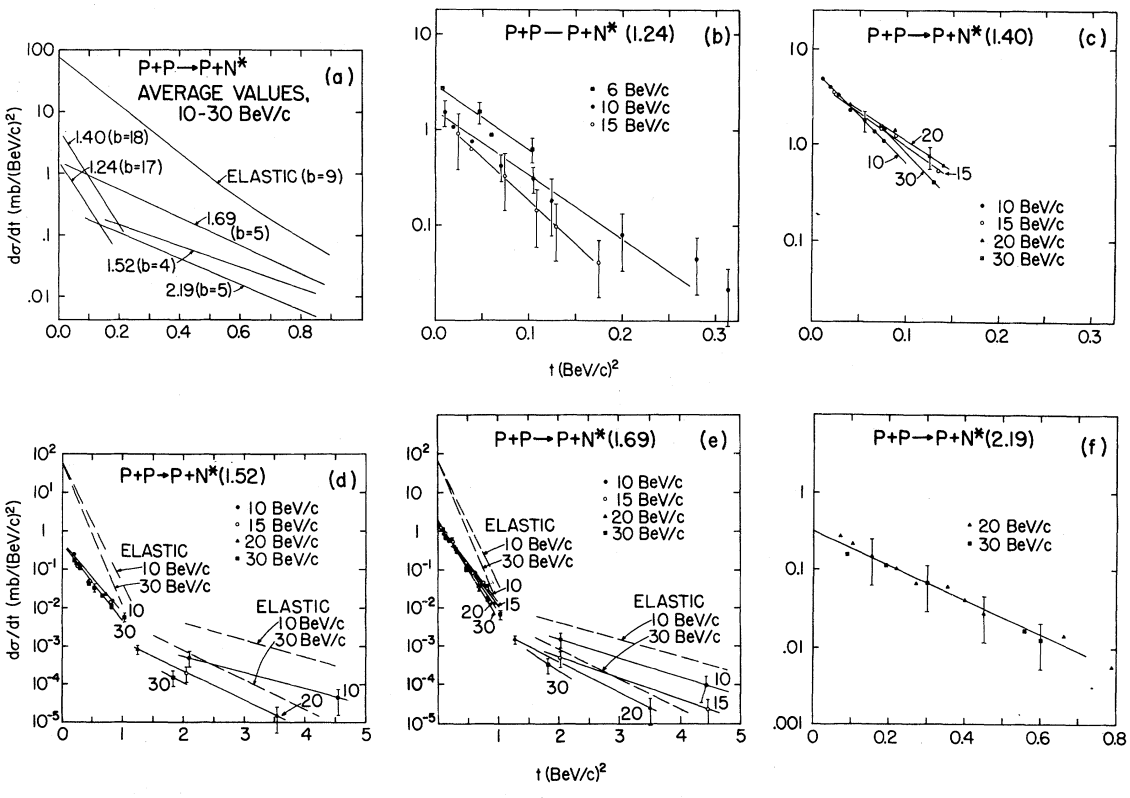

FIG. 3. Comparison of the behavior as a function of $|t|$ of the differential cross sections for the production of the five isobars and for elastic scattering in the region $|t| < 1$ $(\mathrm{BeV}/c)^2$. For each process, $d\sigma/dt = A \exp(-b|t|)$ is plotted versus $|t|$ using the values of A and b from Table I. Relative errors are shown. (a) Average values. (b)-(f) Differential cross sections for the production of the five isobars of mass 1.24, 1.40, 1.52, 1.69, and 2.19 BeV as a function of $|t|$ over a range of incident proton momentum from 6 to 30 BeV/c. The curves are the fits to the data and are given by the parameters in Table I.

Table I. Results of fitting an expression $Ae^{-b|t|}$ to the measured cross sections. For each inelastic channel at each energy we give the range of t used in the fitting, the results A and b, and the total cross section, approximated by $2A/b$.

P_{inc} (BeV/c)	t range (BeV/c)^2	A [mb (BeV/c)$^{-2}$]	b (BeV/c)$^{-2}$	σ (mb)
		$p+p \rightarrow p+N^*(1.238)$		
6	0.01-0.11	2.96 ± 0.56	15.8 ± 2.9	0.376 ± 0.076
10	0.01-0.13	1.60 ± 0.50	17.3 ± 2.0	0.184 ± 0.050
15	0.02-0.13	1.50 ± 1.00	21.1 ± 4.4	0.142 ± 0.100
		$p+p \rightarrow p+N^*(1.40)$		
10	0.01-0.11	6.06 ± 1.00	22.3 ± 3.4	0.544 ± 0.090
15	0.02-0.14	4.80 ± 0.90	15.9 ± 2.3	0.602 ± 0.106
20	0.02-0.14	4.75 ± 1.20	14.4 ± 2.5	0.660 ± 0.150
30	0.07-0.13	8.82 ± 4.20	23.5 ± 5.1	0.744 ± 0.350
		$p+p \rightarrow p+N^*(1.52)$		
10	0.3-0.8	0.39 ± 0.12	3.95 ± 0.51	0.196 ± 0.056
15	0.2-0.9	0.31 ± 0.07	3.88 ± 0.45	0.160 ± 0.032
20	0.2-0.9	0.33 ± 0.07	3.83 ± 0.37	0.170 ± 0.030
30	0.2-0.9	0.36 ± 0.10	4.30 ± 0.50	0.166 ± 0.042
		$p+p \rightarrow p+N^*(1.69)$		
10	0.01-0.8	1.28 ± 0.10	4.50 ± 0.50	0.562 ± 0.058
15	0.02-0.6	1.61 ± 0.17	5.05 ± 0.38	0.638 ± 0.068
20	0.04-0.8	1.47 ± 0.20	5.25 ± 0.48	0.560 ± 0.070
30	0.07-0.9	1.79 ± 0.29	6.19 ± 0.50	0.576 ± 0.084
		$p+p \rightarrow p+N^*(2.19)$		
20	0.07-0.8	0.328 ± 0.072	5.14 ± 0.56	0.128 ± 0.024
30	0.08-0.6	0.274 ± 0.100	5.07 ± 0.90	0.108 ± 0.036

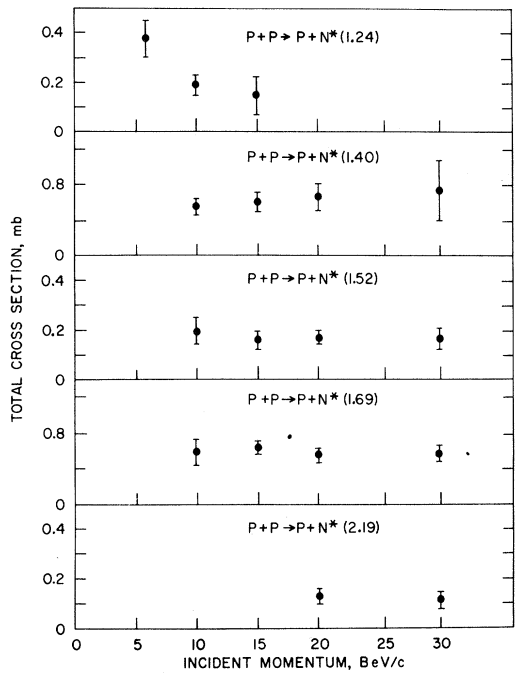

FIG. 4. Total cross sections for the processes $p+p \rightarrow p+N^*$ as a function of the incident proton momentum where N^* is one of the five nucleon isobars of mass 1.24, 1.40, 1.52, 1.69, or 2.19 BeV.

(4) There is essentially no energy dependence in the differential cross sections for $|t|<1$ (BeV/c)^2. [It is interesting that the real part of the elastic differential p-p cross section, measured near $|t| \approx 0.002$ (BeV/c)^2, also has no significant energy dependence.[14]] As a result, the total cross sections, which depend almost entirely on the small angle scattering, are also substantially energy-independent, as can be seen in Fig. 4. The sole exception is the total cross section for $N^*(1.24)$ production, which decreases by approximately a factor of 3 in going from 6 to 15 BeV/c. The general lack of energy dependence is inconsistent with statistical arguments which suggest that since the number of channels increases rapidly with energy, the cross section allotted to any particular channel must decrease with increasing energy. These results indicate, rather, that the channels that are significant at low energies retain their share of the total cross section as the energy increases.

(5) The sum of the total cross sections for the five channels studied amounts to ~1.7 mb, or 6% of the total inelastic p-p cross section (30 mb). Since these channels are only a small

fraction of the possible two-body final states available (e.g., double isobars) this suggests that even at 30 BeV, an appreciable fraction of the total p-p inelastic cross section proceeds via two-body final states.

It is a pleasure to acknowledge the collaboration of Y. Prokoshkin during the early stages of this experiment and the assistance of S. Heller in the programming, of W. Higinbotham, J. Fischer, H. Pate, and J. Jacobs in the construction of the wire planes and electronics, and of E. Bihn and R. Rothe who helped in many aspects of the preparation and running of the experiment. The cooperation of G. K. Green, J. R. Sanford, and the AGS staff was invaluable before and during the experiment.

---

*Work performed under the auspices of the U. S. Atomic Energy Commission.

†Present address: Institute for Nuclear Study, University of Tokyo, Tokyo, Japan.

[1]G. B. Chadwick et al., Phys. Rev. 128, 1823 (1962).

[2]C. M. Ankenbrandt et al., Nuovo Cimento 35, 1052 (1965).

[3]G. Cocconi et al., Phys. Letters 8, 134 (1964).

[4]The isospin and spin quoted are those traditionally assigned to these resonances. Recent phase-shift analyses suggest that there may be additional states resonating at these energies. See, for example, A. Donnachie et al., Phys. Letters 19, 146 (1965).

[5]A brief description was presented by E. Bleser et al. at the Purdue Conference on Instrumentation for High Energy Physics, Purdue University, 12-14 May 1965, IEEE Trans. Nucl. Sci. NS12, 227, 231 (1965). For a more complete description see Brookhaven National Laboratory Report No. BNL 9897 (unpublished); and to be published.

[6]A. N. Diddens, E. W. Jenkins, T. F. Kycia, and K. F. Riley, Phys. Rev. Letters 10, 262 (1963).

[7]G. Bellettini et al., Phys. Letters 18, 167 (1965).

[8]The elastic cross section is drawn from our own data; from K. J. Foley et al., Phys. Rev. Letters 15, 45 (1965); from D. Harting et al., Nuovo Cimento 38, 60 (1965); and from G. Cocconi et al., Phys. Rev. 138, B165 (1965).

[9]For example, L. D. Roper, Phys. Rev. Letters 12, 340 (1964); P. Bareyre, C. Bricman, and G. Villet, Phys. Rev. Letters 14, 881 (1965); P. Auvil, C. Lovelace, A. Donnachie, and A. T. Lea, Phys. Letters 12, 76 (1964); J. Cence, Phys. Letters 20, 306 (1966).

[10]S. D. Drell and K. Hiida, Phys. Rev. Letters 7, 199 (1961).

[11]N. Byers and C. N. Yang, Phys. Rev. 142, 976 (1966).

[12]A. Białas, Phys. Letters 19, 604 (1965).

[13]T. T. Wu and C. N. Yang, Phys. Rev. 137, B708 (1965).

[14]G. Bellettini et al., Phys. Letters 14, 164 (1965); K. J. Foley et al., Phys. Rev. Letters 14, 74 (1965).

ANGULAR DISTRIBUTION OF THE π^0 IN THE REACTION $\pi^+ + p \to \pi^+ + p + \pi^0$ UP TO 1070 MeV

J. F. Detoeuf, Y. Ducros, J. P. Merlo, A. V. Stirling,* B. Thevenet, L. van Rossum, and J. Zsembery†

Département de Physique des Particules Elémentaires, Centre d'Etudes Nucléaires de Saclay, Gif-sur-Yvette, Seine et Oise, France

(Received 1 March 1966)

The differential cross section for the emission of γ rays in $\pi^+ p$ scattering has been measured at five angles and for incident-pion kinetic energies ranging from 500 to 1400 MeV. In a previous paper we have reported the results concerning the total cross section of the process $\pi^+ + p \to \pi^+ + p + \pi^0$.[1]

Let us describe the experimental arrangement and the principle of the analysis of the experimental results. The counter assembly consisted of three distinct groups (Fig. 1): the incident telescope T, the counters surrounding the target C, and the photon telescopes γ, $(\bar{A}S)_i$. Two groups of five telescopes for photon detection were placed symmetrically on either side of the target, in the horizontal plane. Each of

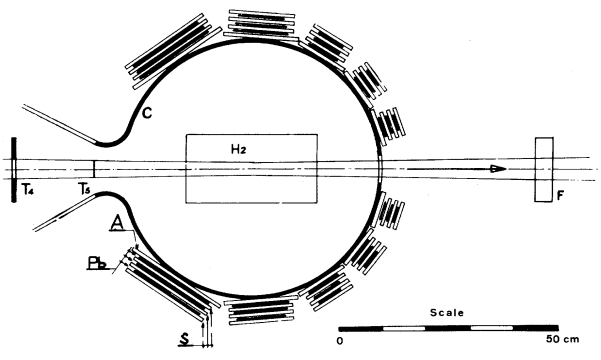

FIG. 1. Arrangement of the counters. $T_1T_2T_3\bar{T}_4T_5\bar{F}$: incident telescope; C: 4π scintillators surrounding the target; $(\bar{A}S)_i$: photon telescope.